

## Effect of UV Irradiation on Apatite Deposition on Anodised TiO<sub>2</sub> Coating Formed Under Mixed Acid Solution

S.S.SALEH<sup>1,a</sup>, M.R. Mohamed YUNUS<sup>1,b</sup> and H.Z.ABDULLAH<sup>1,c\*</sup>

<sup>1</sup>Department of Materials Engineering and Design, Faculty of Mechanical and Manufacturing Engineering, Universiti Tun Hussein Onn Malaysia 86400 Parit Raja, BatuPahat, Johor, Malaysia.

<sup>a</sup>hd120047@siswa.uthm.edu.my, <sup>b</sup>radzi@uthm.edu.my, <sup>c</sup>hasan@uthm.edu.my

**ABSTRACT.** Anodic oxidation method is used to produce thick TiO<sub>2</sub> coating layer in a mixture of acids electrolyte to modify the TiO<sub>2</sub> which is naturally formed on Ti with only few nanometers thick and inert. The TiO<sub>2</sub> coating is then underwent in vitro test to evaluate their bioactivity in simulation body fluid (SBF). In the present work, oxide coatings of TiO<sub>2</sub> were formed on Ti-Cp foil under potentials of 150V at current density of 100 mA.cm<sup>-2</sup> for 10 min. Multiple characterization techniques were used. X-ray diffraction (XRD) is used to obtain mineralogical phase. Scanning electron microscope (SEM) is used to obtain surface morphology. Chemical absorption of the apatite precipitation was tested by using Fourier transform infrared spectroscopy (FT-IR). Surface morphology from the results shows an increased porosity with smaller pore size for TiO<sub>2</sub> formed in mixed acids with higher molar concentration. According to in vitro results it was concluded that apatite precipitation was higher on TiO<sub>2</sub> coatings with increased Ti-O<sup>-</sup> functional groups formed using UV.

**Keywords:** Titanium oxide, Anodic oxidation, UV, Simulation body fluid, Bioactivity;

**Received:** 15.10.2017, **Revised:** 15.12.2017, **Accepted:** 30.02.2018, and **Online:** 20.03.2018;

**DOI:** 10.30967/ijcrset.1.S1.2018.88-94

*Selection and/or Peer-review under responsibility of Advanced Materials Characterization Techniques (AMCT 2017), Malaysia.*

### 1. INTRODUCTION

TiO<sub>2</sub> has shown to exhibit strong physicochemical bonding between Ti implant and living bone because of its ability to induce bone-like apatite in body environment [1]. TiO<sub>2</sub> has three crystalline forms such as anatase, rutile and brookite [2] that may present both amorphous and crystalline structures, depending on process parameters. Crystalline oxides, that is, anatase and rutile present several distinctive features, such as photocatalytic behaviour, superhydrophilicity and biocompatible properties [3].

To improve Ti bioactivity, several surface-modifying techniques have been applied, such as chemical treatment, thermal treatment, electrochemical treatment and anodisation methods [4]. Anodic oxidation method is considered one of the most attractive methods for modifying Ti implant surface [3]. Anodic oxidation can form porous and relatively firm TiO<sub>2</sub> layer on Ti which is highly beneficial for the biological performance of the implant [5]. Anodic oxidation of Ti allows the controlled production of a protective oxide surface layer much thicker than that formed naturally. These coatings may be dense or porous, amorphous or crystalline, depending on the conditions, such as electrolyte type, solution concentration, and applied potential [6]. The electrolytes most commonly used to anodise Ti are sulphuric acid H<sub>2</sub>SO<sub>4</sub> and phosphoric acid H<sub>3</sub>PO<sub>4</sub> [7]. Those aqueous electrolytic solutions which contains modifying elements in the form of dissolved salts which is phosphorous (P) and/or sulfate (S) that incorporate into the resulting TiO<sub>2</sub> coating.

Further improvement of biocompatibility of Ti for orthopaedic and dental applications is endeavoured through the development of bone-like apatite (hydroxyapatite HA) coating on TiO<sub>2</sub> interface [8]. It was found

that physico-chemical bonding between the metallic implant and living bones could be achieved by the formation of a HA in the body environment [9]. The bioactivity of a material can be predicted from the apatite formation in simulation body fluid (SBF), where the existence of phosphorous, calcium, and/or oxygen on anodised sample indicates that HA has grown on that material.

Recent studies have reported the enhanced of apatite formation ability using UV irradiation on TiO<sub>2</sub> [10]. This is due to the photocatalytic ability of TiO<sub>2</sub> which can be excited with UV irradiation. During immersion in SBF the UV promotes cluster hydroxyapatite (HA) precipitation instead of homogenous HA thin film in the case of dark condition [11].

This work evaluates the formation of HA on TiO<sub>2</sub> formed by anodic oxidation. The impact of anodic oxidation parameters on the formation of HA on TiO<sub>2</sub> using SBF under UV will also be studied.

## 2. MATERIALS AND METHODS

**2.1 Sample Preparation.** Commercially-pure Ti (Cp-Ti) foils of dimensions 25 mm x 10 mm x 0.05 mm were wet hand-polished using 1200 grit (~1 μm) abrasive paper, followed by immersion in an ultrasonic bath with acetone, rinsing with distilled water, and dried in air.

**2.2 Anodic Oxidation.** Anodic oxidation was done in an electrochemical cell containing ~0.4 L of diluted mixed aqueous solutions; H<sub>3</sub>PO<sub>4</sub> (Bendosen, 85 wt.%) and H<sub>2</sub>SO<sub>4</sub> (Q-rec, 98 wt.%). The anode and cathode were Ti foil and the anodizing was done with a programmable power supply (Gen 750W/1500W, TDK-Lambda). The anodized foils were cleaned using autoclave and stored in distilled water. The associated experimental parameters are shown in Table 1.

**Table 1** Parameters used for anodic oxidation in H<sub>2</sub>SO<sub>4</sub> and H<sub>3</sub>PO<sub>4</sub> solutions.

Parameters	Value
Temperature (°C)	25
Electrolyte concentration (M)	0.1 M H <sub>2</sub> SO <sub>4</sub>
	2.0 M H <sub>2</sub> SO <sub>4</sub>
	0.1 M H <sub>3</sub> PO <sub>4</sub>
	2.0 M H <sub>3</sub> PO <sub>4</sub>
	0.1 M H <sub>2</sub> SO <sub>4</sub> + 0.1 M H <sub>3</sub> PO <sub>4</sub>
	0.1 M H <sub>2</sub> SO <sub>4</sub> + 2.0 M H <sub>3</sub> PO <sub>4</sub>
	2.0 M H <sub>2</sub> SO <sub>4</sub> + 0.1 M H <sub>3</sub> PO <sub>4</sub>
DC Voltage (V)	150
Current Density (mA.cm <sup>-2</sup> )	100
Duration (min)	10

**2.3 Apatite Formation Evaluation.** After anodic oxidation process, TiO<sub>2</sub> coating samples were subjected to in vitro test where they were immersed in SBF (1.5 M) at 36.5°C in a water bath under irradiation of UV mercury lamp (Cole-Parmer®, wavelength 365 nm, 9 W/cm<sup>2</sup>) for 6 days. SBF were prepared according to Kokubo method [12]. The apatite formation was then evaluated using SEM, XRD, EDX and FTIR.

**2.4 Characterization.** The mineralogical phases of the coatings were determined using (1) X-ray diffraction (XRD, PANalytical X'Pert<sup>3</sup> Powder), (2) the surface morphology were examined using a scanning electron microscope (SEM, Hitachi SUI510) at accelerating voltage of 15 kV, (3) Elemental analyses were done using attached Energy dispersive spectrometer (EDS) (Horiba EmaxX-act®) and (4) the chemical absorption of the apatite precipitation were tested using Fourier transform infrared spectroscopy (FTIR, Perkin-Elmer Spectrum 100).

### 3. RESULTS AND DISCUSSION

Phase mineralogical analysis of TiO<sub>2</sub> coatings produced by individual and mixed acids solutions are shown in Figs. 1 and 2 anatase (TiO<sub>2</sub>, JCPDS card #00-021-1272) and rutile (TiO<sub>2</sub>, JCPDS card #01-072-7374) crystalline can be observed. TiO<sub>2</sub> crystalline phases (anatase and rutile) can be observed on TiO<sub>2</sub> formed under H<sub>2</sub>SO<sub>4</sub> solution, and mixture solution with higher H<sub>2</sub>SO<sub>4</sub> concentration (Fig 1). While TiO<sub>2</sub> coatings formed under H<sub>3</sub>PO<sub>4</sub> solution and mixture solution with higher H<sub>3</sub>PO<sub>4</sub> concentration have observed amorphous structure (Fig. 2).

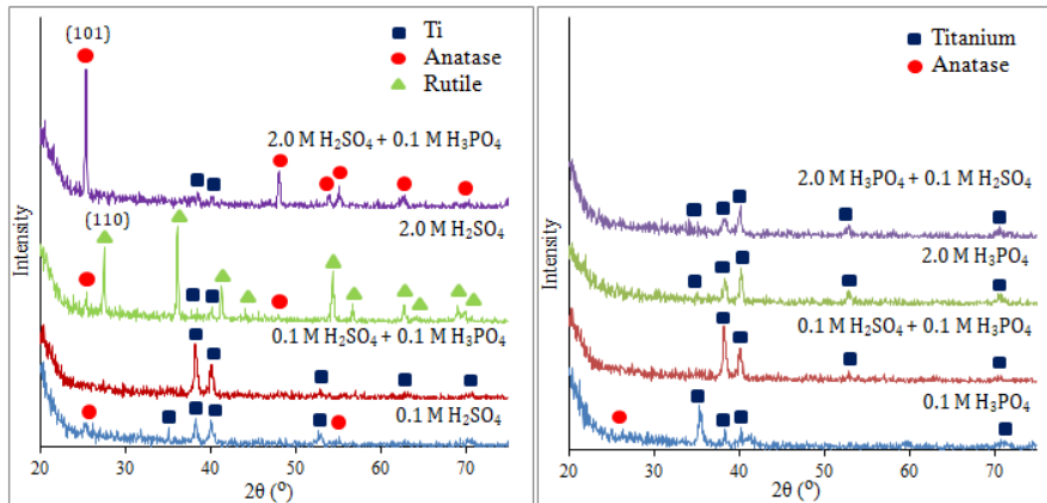


Fig. 1: Phase mineralogical analysis of TiO<sub>2</sub> anodised in 0.1 M H<sub>2</sub>SO<sub>4</sub>, 2.0 M H<sub>2</sub>SO<sub>4</sub>, 0.1 M H<sub>2</sub>SO<sub>4</sub> + 0.1 M H<sub>3</sub>PO<sub>4</sub> and 2.0 M H<sub>2</sub>SO<sub>4</sub> + M H<sub>3</sub>PO<sub>4</sub> at current density 100 mA.cm<sup>-2</sup>

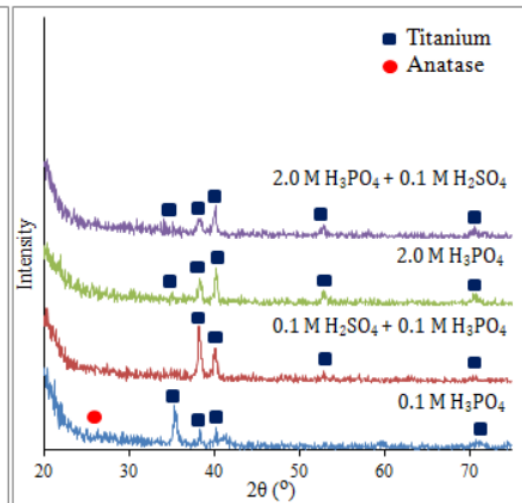


Fig. 2: Phase mineralogical analysis of TiO<sub>2</sub> anodised in 0.1 M H<sub>3</sub>PO<sub>4</sub>, 2.0 M H<sub>3</sub>PO<sub>4</sub>, 0.1 M H<sub>2</sub>SO<sub>4</sub> + 0.1 M H<sub>3</sub>PO<sub>4</sub> and 2.0 M H<sub>3</sub>PO<sub>4</sub> + 0.1 M H<sub>3</sub>PO<sub>4</sub> at current density 100 mA.cm<sup>-2</sup>

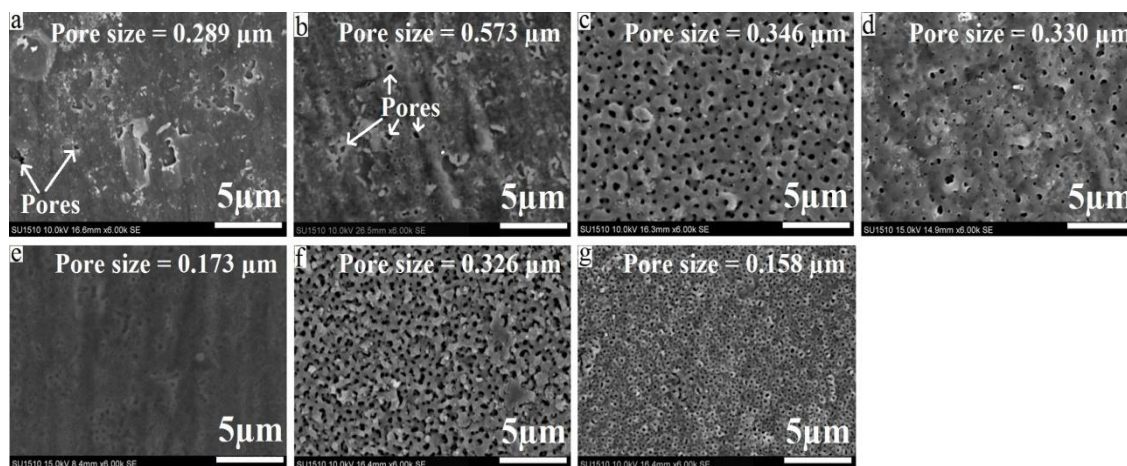
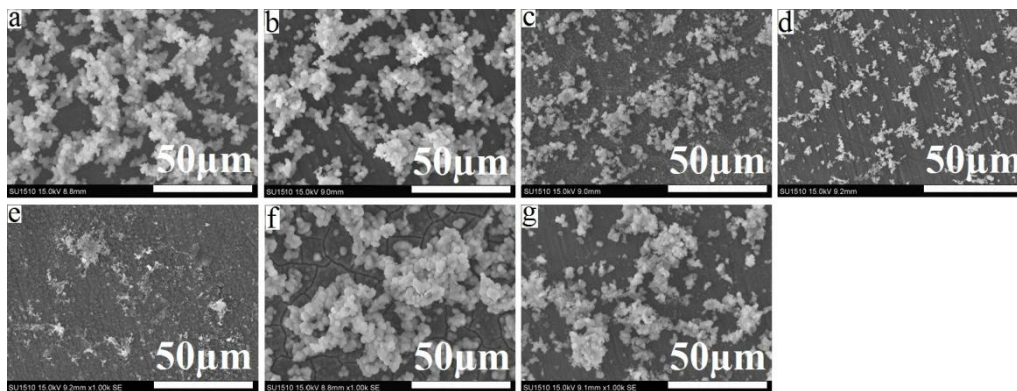


Fig. 3 Surface morphology of TiO<sub>2</sub> film surfaces obtained as follows: (a) 0.1 M H<sub>2</sub>SO<sub>4</sub>, (b) 0.1 M H<sub>3</sub>PO<sub>4</sub>, (c) 2.0 M H<sub>2</sub>SO<sub>4</sub>, (d) 2.0 M H<sub>3</sub>PO<sub>4</sub>, (e) 0.1 M H<sub>2</sub>SO<sub>4</sub> + 0.1 M H<sub>3</sub>PO<sub>4</sub>, (f) 2.0 M H<sub>2</sub>SO<sub>4</sub> + 0.1 M H<sub>3</sub>PO<sub>4</sub> and (g) 2.0 M H<sub>3</sub>PO<sub>4</sub> + 0.1 M H<sub>2</sub>SO<sub>4</sub> at current density 100 mA.cm<sup>-2</sup>

It can be noticed that the surface morphology at lower molarity (0.1 M Fig. 3 (a and b)) at both electrolytes has unorganized surface structure, where some areas has pores and others don't. While the structure at higher molarity and mixed acids have obtained organized surface porosity (Fig. 3 (c-g)). The

porosity at 2.0 M  $H_2SO_4$  (Fig. 3 (c)) take donut-like shape while it take flat shaped pores at 2.0 M  $H_3PO_4$  (Fig. 3 (d)) and its average pores size is lower than the average size of the pores at 2.0 M  $H_2SO_4$ . However, the porosity takes sponge-like shape at mixed electrolyte (2.0 M  $H_2SO_4$  + 0.1 M  $H_3PO_4$ ) (Fig. 3 (f)), while it takes volcano-like shape at 0.1 M  $H_2SO_4$  + 2.0 M  $H_3PO_4$  (Fig. 3 (g)). In general, it can be noticed the average pore size of the coatings anodized in mixed electrolytes is lower than their corresponding at individual electrolytes.

According to in vitro results under UV irradiation in SBF the apatite precipitation on  $TiO_2$  was obtained as shown in Fig. 4. It can be seen that apatite precipitation was in a form of clusters. This is due to the increased formation of Ti-O $\cdot$  functional groups on  $TiO_2$  surface that induce  $Ca^{2+}$  ions which is believed to be caused by UV. This phenomenon has been explained by [13]. Apatite formation was highly obtained on Fig. 4 (a, b, f and g), which corresponds to apatite formed on  $TiO_2$  anodised in low molar solutions and mixed solution with higher molarity.



**Fig. 4** Surface morphology of  $TiO_2$  surfaces immersed for 6 days in SBF under UV is obtained as follows: (a) 0.1 M  $H_2SO_4$ , (b) 0.1 M  $H_3PO_4$ , (c) 2.0 M  $H_2SO_4$ , (d) 2.0 M  $H_3PO_4$ , (e) 0.1 M  $H_2SO_4$  + 0.1 M  $H_3PO_4$ , (f) 2.0 M  $H_2SO_4$  + 0.1 M  $H_3PO_4$  and (g) 2.0 M  $H_3PO_4$  + 0.1 M  $H_2SO_4$  at current density  $100 \text{ mA}\cdot\text{cm}^{-2}$

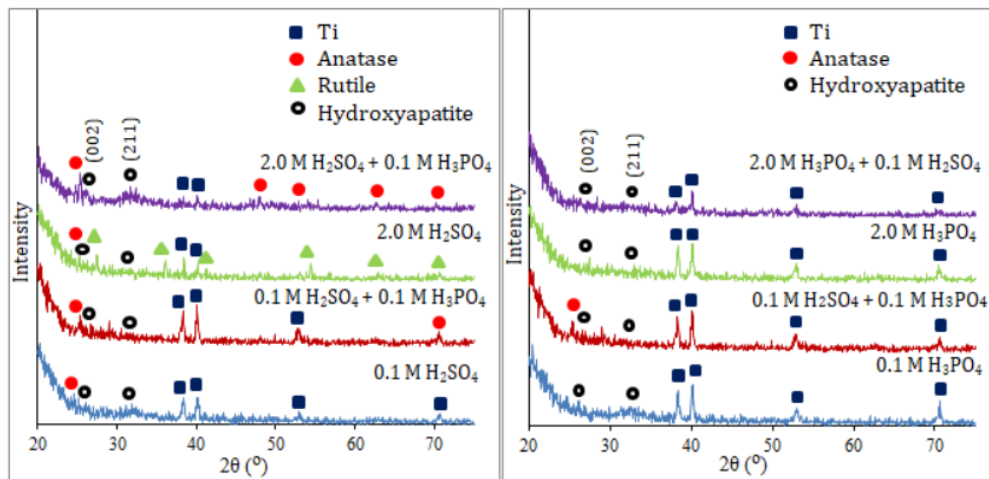


**Fig. 5:** Phase mineralogical analysis of  $TiO_2$  surfaces immersed for 6 days in SBF under UV in 0.1 M  $H_2SO_4$ , 2.0 M  $H_2SO_4$ , 0.1 M  $H_2SO_4$  + 0.1 M  $H_3PO_4$  and 2.0 M  $H_2SO_4$  + 0.1 M  $H_3PO_4$  at current density  $100 \text{ mA}\cdot\text{cm}^{-2}$

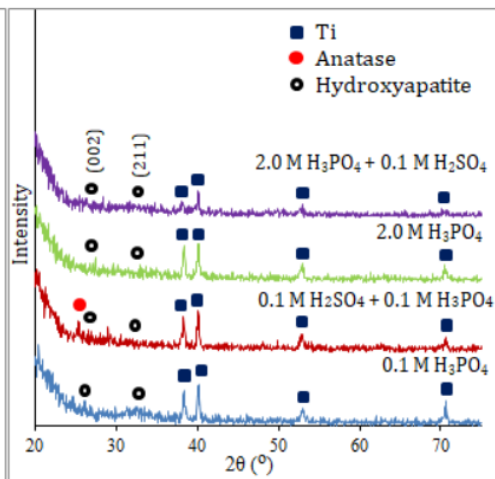


**Fig. 6:** Phase mineralogical analysis of  $TiO_2$  surfaces immersed for 6 days in SBF under UV in 0.1 M  $H_3PO_4$ , 2.0 M  $H_3PO_4$ , 0.1 M  $H_2SO_4$  + 0.1 M  $H_3PO_4$  and 2.0 M  $H_3PO_4$  + 0.1 M  $H_2SO_4$  at current density  $100 \text{ mA}\cdot\text{cm}^{-2}$

However, these coatings have different mineral composition as seen in Figs. 1 and 2 and different surface morphology as obtained in Fig. 3. This can be related to the Ti-O<sup>-</sup> functional groups formed using UV. Phase mineralogical analysis spectra has confirmed the formation of crystalline apatite (HA, JCPDS card #00-055-0592) on all TiO<sub>2</sub> coatings surface as shown in Figs. 7 and 8. Peaks oriented at (002) and (211) were higher on TiO<sub>2</sub> anodised in 0.1 M H<sub>2</sub>SO<sub>4</sub>, 0.1 M H<sub>3</sub>PO<sub>4</sub> and 2.0 M H<sub>2</sub>SO<sub>4</sub> + 0.1 M H<sub>3</sub>PO<sub>4</sub>. These results are in a good agreement with the surface morphology results in Fig. 4. Which promote that higher apatite precipitation obtained higher HA crystalline.

Absorption spectra for TiO<sub>2</sub> as shown as Figs. 7 and 8 have a presence of sulfone (S=O) at band 1300-1350 cm<sup>-1</sup> on TiO<sub>2</sub> anodised in H<sub>2</sub>SO<sub>4</sub> solution and phosphine (P-H) at band 950-1200 cm<sup>-1</sup> was obtained on TiO<sub>2</sub> anodised in H<sub>3</sub>PO<sub>4</sub>. Both sulfone and phosphine were obtained on TiO<sub>2</sub> anodised in mixed solutions. Hydroxyl groups (OH) stretching region 3100-3400 cm<sup>-1</sup> except for TiO<sub>2</sub> anodised in 2.0 M H<sub>3</sub>PO<sub>4</sub> and Ti-OH at band 3635, 3645, 3680, 3750 and 3840 cm<sup>-1</sup> was also obtained on all the coatings. Water (H<sub>2</sub>O) at band 1860 cm<sup>-1</sup> was also obtained on all the coatings, especially in coatings anodised in higher H<sub>2</sub>SO<sub>4</sub> concentration and in mixed solution with higher H<sub>2</sub>SO<sub>4</sub>, which obtained stronger water absorption band. This can be due to the water trapped inside the grooves on their complicated porous structure (Fig. 3).

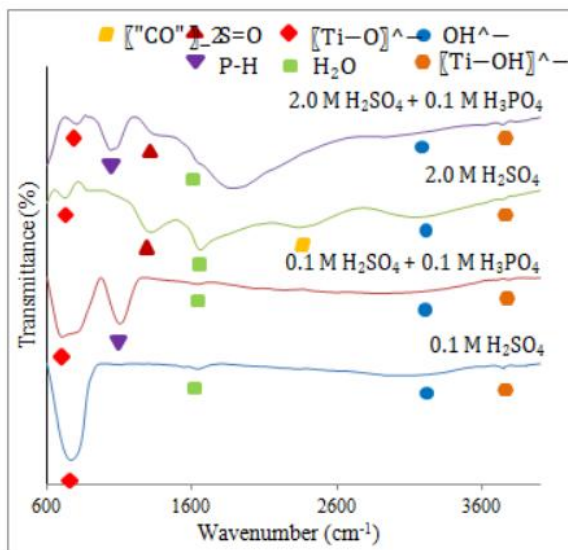


Fig. 7: Absorption analysis of TiO<sub>2</sub> surfaces anodised in 0.1 M H<sub>2</sub>SO<sub>4</sub>, 2.0 M H<sub>2</sub>SO<sub>4</sub>, 0.1 M H<sub>2</sub>SO<sub>4</sub> + 0.1 M H<sub>3</sub>PO<sub>4</sub> and 2.0 M H<sub>2</sub>SO<sub>4</sub> + 0.1 M H<sub>3</sub>PO<sub>4</sub> current density 100 mA.cm<sup>-2</sup>

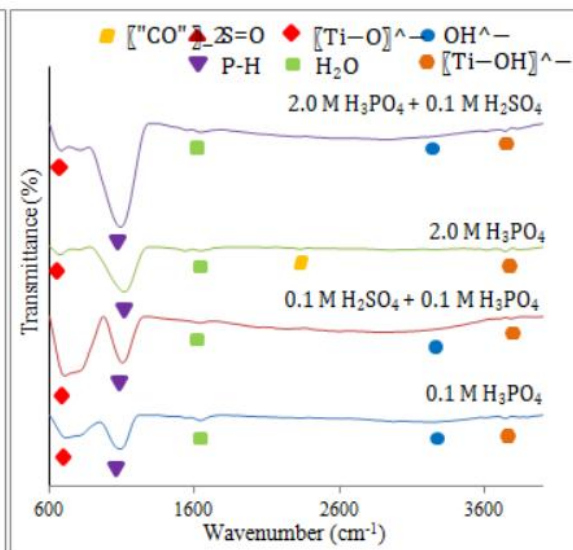


Fig. 8: Absorption analysis of TiO<sub>2</sub> surfaces anodised in 0.1 M H<sub>3</sub>PO<sub>4</sub>, 2.0 M H<sub>3</sub>PO<sub>4</sub>, 0.1 M H<sub>2</sub>SO<sub>4</sub> + 0.1 M H<sub>3</sub>PO<sub>4</sub> and 2.0 M H<sub>2</sub>SO<sub>4</sub> + 0.1 M H<sub>3</sub>PO<sub>4</sub> current density 100 mA.cm<sup>-2</sup>

Figs. 9 and 10 show absorption spectra for TiO<sub>2</sub> irradiated with UV for 12 hours. It can be seen that Ti-O<sup>-</sup> functional group stretching has increased on all the coatings after exposed to UV. This has happened because TiO<sub>2</sub> (anatase) display photocatalytic activity under UV. Therefore, results in a formation of hydroxide groups [15]. Ti-OH groups then react with OH<sup>-</sup> to form Ti-O<sup>-</sup> groups [14]. This could be related to the sharp stretching of Ti-OH at band 1100 cm<sup>-1</sup> as seen in Fig. 9 for anatase crystalline TiO<sub>2</sub> coated anodised in 2.0 M H<sub>2</sub>SO<sub>4</sub> + 0.1 M H<sub>3</sub>PO<sub>4</sub>. It can be noticed that higher apatite formation has been resulted on coatings anodised in 0.1 M H<sub>3</sub>PO<sub>4</sub>, 0.1 M H<sub>2</sub>SO<sub>4</sub> and 2.0 M H<sub>2</sub>SO<sub>4</sub> + 0.1 M H<sub>3</sub>PO<sub>4</sub> as seen in Fig. 4 according to surface morphology. Along with higher HA crystallinity as resulted in Figs. 5 and 6 according to the phase mineralogy. This is can be related to larger Ti-O<sup>-</sup> stretching as obtained in coatings anodised in 0.1 M H<sub>3</sub>PO<sub>4</sub> and 2.0 M H<sub>2</sub>SO<sub>4</sub> + 0.1 M H<sub>3</sub>PO<sub>4</sub>. TiO<sub>2</sub> anodised in 0.1 M H<sub>2</sub>SO<sub>4</sub> has originally high Ti-O<sup>-</sup> stretching although it did not obtain significantly larger Ti-O<sup>-</sup> stretching after UV irradiation.

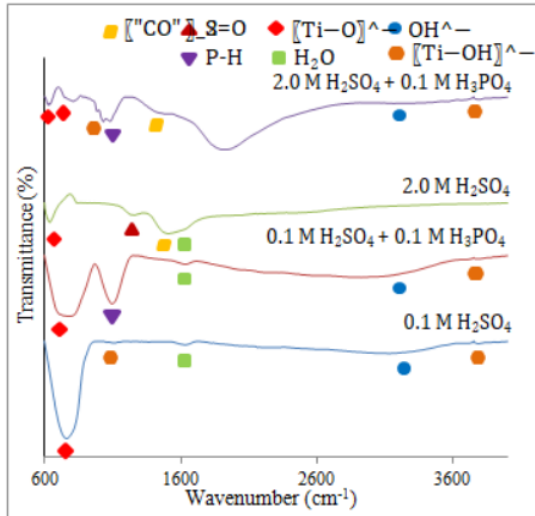


Fig. 9: Absorption analysis of TiO<sub>2</sub> surfaces after 12 hrs of irradiation under UV for TiO<sub>2</sub> anodised in 0.1 M H<sub>2</sub>SO<sub>4</sub>, 2.0 M H<sub>2</sub>SO<sub>4</sub>, 0.1 H<sub>2</sub>SO<sub>4</sub> + 0.1 M H<sub>3</sub>PO<sub>4</sub> and 2.0 M H<sub>2</sub>SO<sub>4</sub> + 0.1 M H<sub>3</sub>PO<sub>4</sub> current density 100 mA.cm<sup>-2</sup>

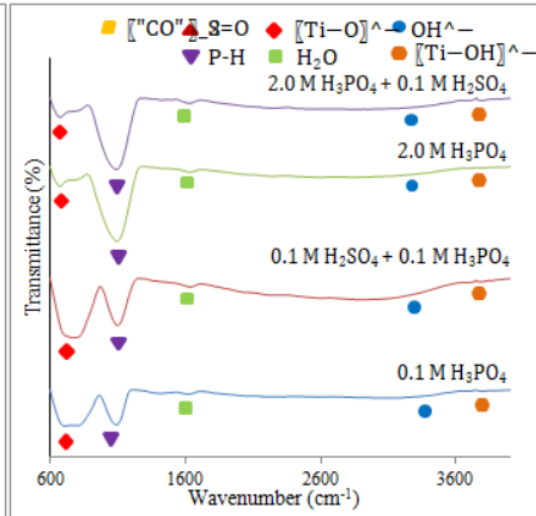


Fig. 10: Absorption analysis of TiO<sub>2</sub> surfaces after 12 hrs of irradiation under UV for TiO<sub>2</sub> anodised in 0.1 M H<sub>3</sub>PO<sub>4</sub>, 2.0 M H<sub>3</sub>PO<sub>4</sub>, 0.1 H<sub>2</sub>SO<sub>4</sub> + 0.1 M H<sub>3</sub>PO<sub>4</sub> and 2.0 M H<sub>3</sub>PO<sub>4</sub> + 0.1 M H<sub>2</sub>SO<sub>4</sub> current density 100 mA.cm<sup>-2</sup>

#### 4. SUMMARY

The effect of UV irradiation on apatite deposition on anodised TiO<sub>2</sub> coating formed under mixed acid solution was successfully investigated. Based on in vitro results it was concluded that apatite precipitation was higher on TiO<sub>2</sub> coatings with increased Ti-O- functional groups formed using UV.

#### ACKNOWLEDGEMENTS

The authors gratefully acknowledge Ministry of Higher Education, Malaysia for the financial support provided for the research through Research Grant Scheme, FRGS vot 1212. Also, a grateful acknowledgment to the Centre for Graduate Studies UTHM for their partly sponsor of this work.

#### REFERENCES

- [1] R. Hazan, R. Brenner, U. Oron, Bone growth to metal implants is regulated by their surface chemical properties, *Biomater.*, 14 (1993) 570-574.
- [2] T. Dikici, M. Erol, M. Toparli, E. Celik, Characterization and photocatalytic properties of nanoporous titanium dioxide layer fabricated on pure titanium substrates by the anodic oxidation process, *Ceram. Int.*, 40 (2014) 1587-1591.
- [3] K.H. Park, S.J. Heo, J.Y. Koak, S.K. Kim, J.B. Lee, S.H. Kim, Y. Lim, Osseointegration of anodized titanium implants under different current voltages: A rabbit study, *J. Oral.Rehab.*, 34(2007a) 517-527.
- [4] Y. Wang, H. Yu, C. Chen, Z. Zhao, Review of the biocompatibility of micro-arc oxidation coated titanium alloys, *Mater. Design*, 85 (2015) 640-652.
- [5] K. Lee, Y.H. Jeong, W.A. Brantley, H.C. Choe, Surface characteristics of hydroxyapatite films deposited on anodized titanium by an electrochemical method, *Thin Solid Films*, 546 (2013) 185-188.
- [6] S.S. Saleh, H.Z. Abdullah, Optimization and characterization of anatase formed on anodized titanium in mixed acids, *ARPN Journal of Engineering and Applied Sciences*, 11 (2016) 9809-9814.
- [7] M.V. Diamanti, M.P. Pedferri, Effect of anodic oxidation parameters on the titanium oxides formation. *Corros. Sci.*, 49 (2007) 939-948.

- [8] K. Hayashi, N. Matsuguchi, K. Uenoyama, T. Kanemaru, Y. Sugioka, Evaluation of metal implants coated with several types of ceramics as biomaterials, *J. Biomed. Mater. Res.*, 23 (1989) 1247-1259.
- [9] E. Milella, F. Cosentino, A. Licciulli, C. Massaro, Preparation and characterisation of titania/hydroxyapatite composite coatings obtained by sol-gel process, *Biomater.*, 22 (2001) 1425-1431.
- [10] H.Z. Abdullah, C.C. Sorrell, Gel Oxidation of Titanium and Effect of UV Irradiation on Precipitation of Hydroxyapatite from Simulated Body Fluid, *Key Eng. Mater.*, 448 (2012) 1229-1237.
- [11] M. Ueda, T. Kinoshita, M. Ikeda, M. Ogawa, Photo-induced formation of hydroxyapatite on TiO<sub>2</sub> synthesized by a chemical-hydrothermal treatment, *Mater. Sci. Eng. C*, 29 (2009) 2246.
- [12] T. Kokubo, H. Takadama, How useful is SBF in predicting in vivo bone bioactivity?, *Biomater.* 27 (2006) 2907-2915.
- [13] Y.P. Guo, H.X. Tang, Y. Zhou, D.C. Jia, C.Q. Ning, Y.J. Guo, Effects of mesoporous structure and UV irradiation on in vitro bioactivity of titania coatings, *Appl. Surf. Sci.*, 256 (2010) 4945-4952.
- [14] M. Ueda, H. Sai, M. Ikeda, M. Ogawa, Formation of hydroxyapatite on titanium oxides in simulated body fluid under UV irradiation, *Mater. Sci. Forum.*, 654-656 (2010) 2257.
- [15] X. Liu, X. Zhao, B. Li, C. Cao, Y. Dong, C. Ding, P.K. Chu, UV-irradiation-induced bioactivity on TiO<sub>2</sub> coatings with nanostructural surface, *Acta Biomater.*, 4 (2008) 544-552.